Effects of a Catalytic Volatile Particle Remover (VPR) on the Particulate Matter Emissions from a Direct Injection Spark Ignition Engine

ARTICLE *in* ENVIRONMENTAL SCIENCE & TECHNOLOGY · SEPTEMBER 2011

Impact Factor: 5.33 · DOI: 10.1021/es2008209 · Source: PubMed

3 AUTHORS, INCLUDING:

Longfei Chen
Beihang University(BUAA)
46 PUBLICATIONS **620** CITATIONS

SEE PROFILE

Environmental Science & Technology

ARTICLE

pubs.acs.org/est

Effects of a Catalytic Volatile Particle Remover (VPR) on the Particulate Matter Emissions from a Direct Injection Spark Ignition Engine

Fan Xu,* Longfei Chen, and Richard Stone

Combustion Engines Group, Department of Engineering Science, University of Oxford, Oxford, United Kingdom

Supporting Information

ABSTRACT: Emissions of fine particles have been shown to have a large impact on the atmospheric environment and human health. Researchers have shown that gasoline engines, especially direct injection spark ignition (DISI) engines, tend to emit large amounts of small size particles compared to diesel engines fitted with diesel particulate filters (DPFs). As a result, the particle number emissions of DISI engines will be restricted by the forthcoming EU6 legislation. The particulate emission level of DISI engines means that they could face some challenges in meeting the EU6 requirement. This paper is an experimental study on the size-resolved particle number emissions from a spray guided DISI engine and the performance of a catalytic volatile particle remover (VPR), as the EU legislation seeks to exclude volatile particles. The performance of the catalytic VPR was evaluated by varying its temperature and the exhaust residence time. The effect of the catalytic VPR acting as an oxidation catalyst on particle emissions was also tested. The results show that the catalytic VPR led to a marked reduction in the number of particles, especially the smaller size (nucleation mode) particles. The catalytic VPR is essentially an oxidation catalyst, and when post three-way catalyst (TWC) exhaust was introduced to the catalytic VPR, the performance of the catalytic VPR was not affected much by the use of additional air, i.e., no significant oxidation of the PM was observed.

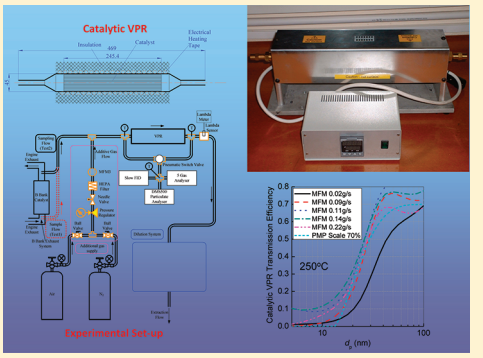

1. INTRODUCTION

With the tightening of emissions legislation, more research concerns the particle emissions from gasoline engines, especially those with direct injection. Recently, much attention has been given to the influence of fine particulate material (PM) in the atmosphere on human health.

Concerns about possible adverse health effects of particles from engines led to a re-examination of PM standards and measurement protocols by Kittelson.[1] The total particle size distribution can be divided into three modes, namely a nucleation mode, an accumulation mode, and a coarse mode. Most of the particle mass exists in the so-called accumulation mode in the 0.1−0.3 μm diameter range. This is where the carbonaceous agglomerates and associated adsorbed materials reside. The nucleation mode typically consists of particles in the 0.005−0.05 μm diameter range. This mode usually consists of volatile organic and sulfur compounds that form during exhaust dilution and cooling, and may also contain solid carbon and metal compounds. The nucleation mode typically contains 1−20% of the particle mass but more than 90% of the particle number.

Various tests have already been carried out on vehicles with different types of engine.[2−6] Generally, it is found that particles are generated during acceleration and cold start in a drive cycle. For port fuel injection gasoline vehicles, after catalyst light-off, particle emissions diminished to near negligible levels at moderate cruise speeds and during deceleration. It has been indicated by various researchers that the PFI and DPF diesel vehicles showed the lowest particulate emissions, while particle emissions from diesel vehicles without DPFs were the highest.[7−9] The level of particle emissions from a DISI vehicle was between that of the PFI and diesel vehicles.[5,6,10−14] DISI engines tend to emit higher levels of particulate emissions during stratified operation.[5,15] It was shown by Ericsson et al.[5] that the difference in particulate number between the homogeneous and the stratified modes was a factor of approximately 40.

Although most research has found that particle number (P_n) emissions from DISI engines were higher than those of DPF-diesel or PFI gasoline engines by an order of magnitude,[5,6,10−14] the research from CONCAWE[16] showed that the P_n emissions from DISI vehicles were of the same order as those from the DPF diesel vehicles over the NEDC cycle. So it is of interest to further investigate the particle emissions from the most recent DISI engines. It is well-known that when a DISI engine operates in stratified lean conditions, it will emit a high number concentration of particles. It can be argued that, during stratified combustion, soot was formed as a partially premixed flame propagated through locally rich zones and from pool fires caused by thin films of liquid fuel on the piston surface.[17−19] However, during stoichiometric operation when using a piezoelectric injector with

Received: March 11, 2011
Accepted: September 8, 2011
Revised: June 14, 2011

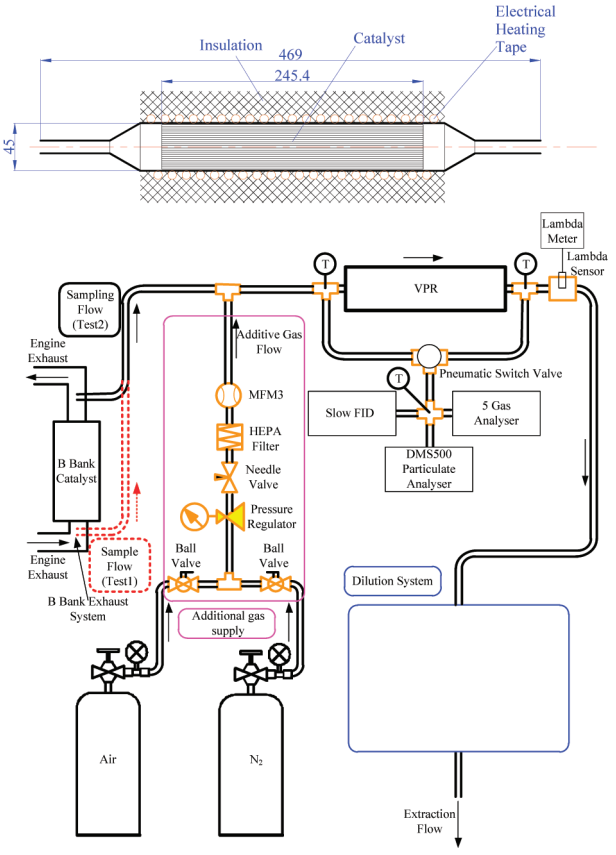

Figure 1. Experimental setup and construction of the catalytic VPR system.

multiple injections in a DISI engine (to further increase homogenization and reduce spray penetration), then the P_n emissions may be lowered. By using turbocharging for downsizing, stoichiometric DISI engines show advantages on fuel economy over turbocharged MPI engines[20] and lowered P_n emission compared with lean DISI engines.

To investigate the characteristics of particle emissions from engines, a catalytic stripper (CS, an oxidation catalyst) has been tested by Kittelson and co-workers.[21,22] It was reported that complete removal of volatile particles could be achieved but that it also led to the removal of 15−25% of the solid particles. This loss has been attributed to thermophoretic deposition caused by cooling after the catalytic stripper. A volatile particle remover (VPR) system is required by the European PMP program.[10,23] The particle loss in the catalytic stripper led to the development of a solid particle sampling system (SPSS)[24] that used dilution immediately after an oxidation catalyst. Khalek[24] presents a comprehensive discussion and analysis of the operation of the SPSS, and characterizes its performance using salt (NaCl), ammonium sulfate, and oil aerosols. The ammonium sulfate decomposed and (as with the oil) led to particle penetration through the SPSS that was always below 10%. In contrast, the penetration of the salt aerosol was, within experimental tolerance, 100%. In a subsequent paper Khalek and Bougher[25] compared the performance of the SPSS using a catalytic stripper (CS, an oxidation catalyst) with an evaporation tube (ET) using particles of tetracontane (as specified in the European PMP). They conclude that the catalytic stripper outperforms the evaporation tube, since the catalytic stripper will oxidize the vaporized hydrocarbons so that there is then no possibility of their recondensation. So, it is of interest to investigate the performance of the catalytic stripper based volatile particle remover system on the PM emissions from a spray guided direct injection (SGDI) engine; previous work has utilized a wall guided direct injection engine.[26] In the work reported here, engine experiments were carried out to study a catalytic volatile particle remover (VPR), and to find out if it can achieve the transmission efficiencies required by the PMP procedures.

2. EXPERIMENTAL APPARATUS

The test engine was a Jaguar naturally aspirated, V8 direct injection spark ignition engine.[27] The main characteristics of the engine are listed in Table S1. During these tests, the spark timing was fixed at 30 °CA (crank angle degree) before compression top dead center. A single injection during the intake stroke at 280 °CA before compression top dead center to generate a nominally homogeneous mixture.

A schematic of the particulate emissions measurement system and the construction of the catalytic VPR system tested in this work are shown in Figure 1. The geometric data for the catalytic VPR system tested in this work are shown in Figure 1, and its performance as an oxidation catalyst is discussed later in the context of Figure S5 (see Supporting Information). The catalytic VPR system consists of a temperature-controlled heated tube with an oxidation catalyst inside. The effects of the VPR temperature and residence time on the catalytic VPR performance were examined.

It can be seen from Figure 1 that in Test 1, the exhaust pre-TWC was drawn into the catalytic VPR. At each test point, the PM emissions pre-VPR and post-VPR were measured using a Cambustion DMS500 particle sizer.[28] The sampling flow rate of the DMS (MFM_{DMS}) was set to 0.02 g/s. A pneumatic switching valve was used to select between pre-VPR and post-VPR. The switching valve was heated by hot air to keep the sampling temperature at around 90 °C, thereby preventing particle formation by condensation. The temperature of the sampling flow pre- and post-VPR, as well as the flow temperature entering DMS, were measured using thermocouples. Downstream of the catalytic VPR, the exhaust flow then entered a dilution/extraction system. As a result, the residence time of the exhaust gas in the catalytic VPR was varied, and the effects of exhaust residence time on PM emissions were studied by means of varying the flow rate of the dilution gas (MFM_{air}) added upstream of the VPR. Also, in this test, the VPR temperature was changed to investigate its effect on the VPR performance. The test conditions are listed in Table 1. The residence time (t_r) is calculated assuming a linear variation in the temperature within the catalytic VPR along its length.

$$\dot{V} = \frac{\dot{m} \times R_s \times (T_1 + T_2)/2}{P} \quad (1)$$

$$t_r = V/\dot{V} \quad (2)$$

where $\dot{V}$ (m^3/s) represents the volume flow rate through the VPR, $\dot{m}$ (g/s) represents the mass flow rate through VPR, R_s ($J \times g^{-1} \times K^{-1}$) represents the specific gas constant of exhaust, T_1 (K) represents the pre-VPR temperature, T_2 (K) represents the post-VPR temperature, P (Pa) represents the exhaust pressure, t_r (s) represents the residence time, and V (m^3) represents the internal volume of the catalytic VPR.

In Test 2, the exhaust was sampled downstream of the TWC (Figure 1). The test procedure was as follows. At each engine

dx.doi.org/10.1021/es2008209 |Environ. Sci. Technol. XXXX, XXX, 000–000

Table 1. Tests Conditions

residence times (s) for test 1					
	$MFM_{exhaust}$/(g/s)				
VPR temperature/°C	0.02	0.09	0.11	0.14	0.22
150	15.9	3.36	2.68	2.05	1.24
250	14.8	3.01	2.35	1.76	1.08
350	13.8	2.98	2.29	1.71	1.02

mass flow of additional gas (g/s) for test 2					
		VPR-DF			
engine Lambda	additional gas	1	1.1	1.2	1.3
1	air	0	0.02	0.04	0.06
	N_2	0	0.02	0.04	0.06
0.9	air	0	0.02	0.04	0.06
	N_2	0	0.02	0.04	0.06

Lambda (actual/stoichiometric air−fuel ratio), supplementary air was first used to study the oxidation effect of the catalytic VPR. By adjusting the needle valve in the additional gas supply route, the mass flow rate of the additional air was controlled to give the Lambda meter reading that was 0.1, 0.2, or 0.3 above the Lambda at which the engine was operating. At each Lambda meter reading, the mass flow rate of the additional gas ($MFM_{add\ gas}$) was measured by MFM 3 and was recorded. Then, the air supply was swapped with nitrogen (N_2) to investigate the dilution effects of additional gas on the PM emissions. At each engine operating point, the needle valve was adjusted to let MFM 3 give the same readings as those recorded in the experiments with additional air. By comparing the two sets of results (additional air against N_2), the oxidation effect and dilution effect of the additional gas can be examined separately. The VPR dilution factor (VPR-DF) is defined as

$$\text{VPR-DF} = 1 + (\text{MFM}_{\text{addgas}}/\text{MFM}_{\text{exhaust}}) \quad (3)$$

where $MFM_{exhaust}$ represents the total mass flow rate of exhaust.

When testing with additional air at stoichiometric conditions, the VPR-DF is the same as the Lambda meter reading. The test point conditions are listed in Table 1.

During the experiments, both the raw data and log-normal fits of DMS signal were logged into the computer for a number of samples. The DMS sampling line was maintained at 80 °C, and internally controlled dilution air was preheated before being mixed with the sample at entry to the sampling line. Before entry to the DMS sampling line, the pipework and pneumatic switching valve were maintained at above 80 °C. A typical sample flow into the DMS was 2 LPM so the residence time in the sampling system is very short (~4 s) so diffusion and thermophoretic losses can be ignored. The DMS log-normal output is generated by a Bayesian statistical algorithm,[29] which separates the nucleation mode from the accumulation mode particles. The DMS output is a matrix containing number concentration at a given sample number (i.e., time) and particle diameter. The number matrix is then converted to a mass matrix by using an empirical equation. The number matrix and mass matrix are averaged to find a mean concentration plot over particle diameter, which can then be integrated to obtain the total number and total mass of particles emitted by the engine. The formula used to calculate particle mass was obtained previously from back-to-back tests with the DMS500 and a centrifugal couette flow particle mass analyzer on the same engine.[30]

$$\text{mass}_{d\text{p}} = 1.72 \times 10^{-24} \times {d_\text{p}}^{2.65} \times n_{d\text{p}} \quad (4)$$

where d_p represents the diameter of the particles (nm), mass_{dp} (kg/cm^3) represents particle mass concentration of diameter d_p, and n_{dp} ($no./cm^3$) represents particle number concentration of diameter d_p. From this equation, it can be seen that the larger particles contribute much more to the particle mass than smaller particles. The log-normal fitting is particularly useful as it eliminates the noise at both the high and low ends of the measured raw spectrum. As a result, it is more appropriate to use log-normal fitted data in calculating particle mass distributions from the particle size distribution than to use raw data.

European legislation requires the particle number emissions measurement equipment to have counting efficiencies of 50% (±12%) at particle sizes of 23 nm (±1 nm) and of >90% at 41 nm (±1 nm) electrical mobility diameters.[23] During data postprocessing, a digital filter using a Wiebe function was applied to the raw measurement data to simulate this legislation requirement for the counting efficiency. The formula for the filter is as follows.

$$f = 1 - \exp\left[-3.54\left(\frac{d_\text{p} - 14}{40}\right)^{1.09}\right] \quad (5)$$

where d_p (nm) represents the diameter of the particles.

A plot of the filter is shown in the SI (Figure S1), in which the legislation requirements are plotted with cross points. It can be seen that the counting efficiencies represented by the filter fulfill the legislative requirement.

3. RESULTS AND ANALYSIS

The experimental results are divided into two parts corresponding to the tests described above. The particle measurement results presented here are an average of data measured for 90 s.

Effects of the VPR Temperature and Residence Time on the Catalytic VPR Performance. Figure S2 shows the temperatures of the pre-VPR and post-VPR sample points under different test conditions for engine-out emissions. It can be seen that the temperatures pre- and post-VPR increase as the mass flow rate of the exhaust becomes higher, showing that the mass flow rate of the exhaust extraction affects the temperature at inlet and outlet of the VPR. This is because as the $MFM_{exhaust}$ increases, the velocity of the exhaust becomes higher, which leads to less cooling per unit mass along the copper pipe connecting the engine exhaust pipe to the catalytic VPR.

Figure S3 shows a representative raw size distribution from the DMS data and its log-normal fitting, which was taken pre-VPR with a 250 °C VPR temperature and 0.14 g/s mass flow of exhaust. Symonds et al.[29] gave a very comprehensive discussion of how the bilognormal fit is obtained using Bayesian statistics applied to the original electrometer current measurements. It can be seen that the bilognormal result fits the trend of the raw data very well. As the log-normal fitting is very useful in eliminating the noise in the raw data at both the high and low ends of the particle size range, the log-normal fitting results are used in the following analysis.

The number transmission efficiency across the catalytic VPR is defined as

$$\eta_{d\text{p}} = n_{d\text{p}}(\text{downstream})/n_{d\text{p}}(\text{upstream}) \quad (6)$$

dx.doi.org/10.1021/es2008209 |Environ. Sci. Technol. XXXX, XXX, 000–000

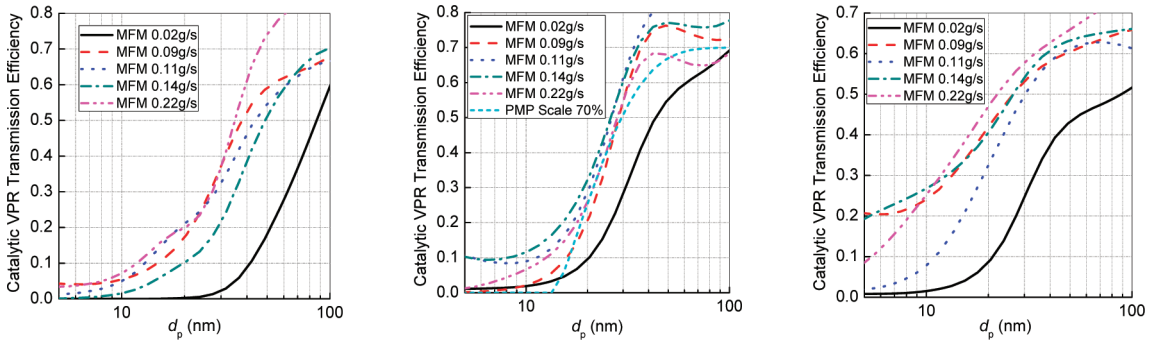

(a) VPR 150°C (b) VPR 250°C (c) VPR 350°C

Figure 2. Number transmission efficiencies versus d_p with different sample flow rates taken from the engine exhaust ($MFM_{exhaust}$) and different VPR temperatures (refer to Table 1) and compared to eq 7.

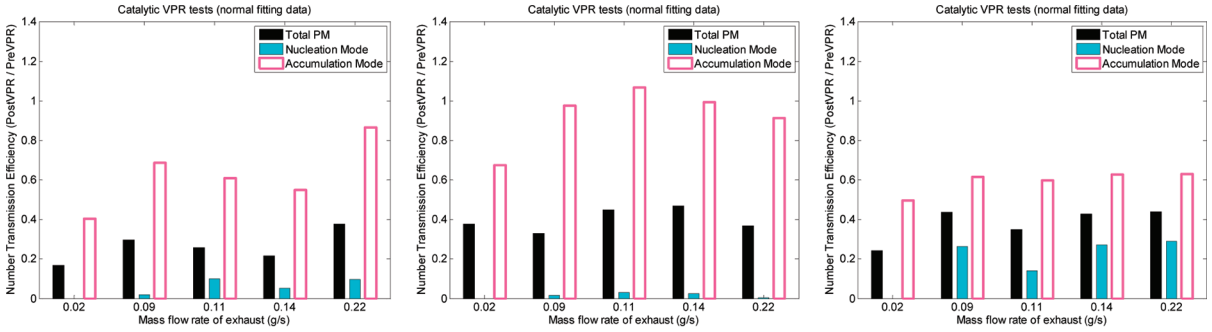

(a) VPR 150°C, Number ratio (b) VPR 250°C, Number ratio (c) VPR 350°C, Number ratio

Figure 3. Number transmission efficiencies for different modes (total, nucleation, and accumulation) for different sample flow rates ($MFM_{exhaust}$) and different VPR temperatures (refer to Table 1).

where η_{dp} represents the transmission efficiency of diameter d_p, n_{dp}(downstream) (no./cm^3) represents particle number concentration of diameter d_p downstream the catalytic VPR, and n_{dp}(upstream) (no./cm^3) represents particle number concentration of diameter d_p upstream the catalytic VPR.

The number transmission efficiencies are shown in Figure 2. It can be seen that the transmission efficiencies increase as the particle size increases. The curves for different VPR temperatures and $MFM_{exhaust}$ are similar, except that the curves for $MFM_{exhaust}$ = 0.02 g/s show relatively lower transmission efficiencies at the low end of the particle size range (<50 nm). Also these results show that the catalytic VPR has more effect on the nucleation mode particles than the accumulation mode particles. In some cases, for example at 250 °C VPR temperature and 0.11 g/s $MFM_{exhaust}$, a sudden rise of the transmission efficiency can be seen at the high end of the particle size range. This is due to noise in the raw DMS data at the high end of the particle size range. Also, it can be seen for particles with d_p > 40 nm the loss is about 30% as the exhaust flows through the catalytic VPR (e.g., Figure 2b). So as to account for the solid particle loss, the catalytic VPR transmission efficiencies can be compared with the 70% scaled PMP counting efficiency (eq 7) as shown in Figure 2b.

$$f = \left(1 - \exp\left[-3.54\left(\frac{d_p - 14}{40}\right)^{1.09}\right]\right) \times 0.7 \qquad (7)$$

where d_p (nm) represents the diameter of the particles.

The PMP specification is for a 50% efficiency at 23 nm, and >90% at 41 nm. Once the $MFM_{exhaust}$ was above 0.09 g/s, the catalytic VPR transmission efficiencies for different size particles showed similar trends with the scaled PMP counting efficiency.

Figure 3 shows the number ratio (post-VPR/pre-VPR) for the total PM, nucleation mode, and accumulation mode. The number reduction ratios of the nucleation mode particles are higher than those of the accumulation mode particles, as their sizes are much smaller than those of the accumulation mode particles. When these results are analyzed in terms of mass (see SI Figure S4), the reduction of total P_m is less than the reduction of total P_n, and the mass ratio of the total particulate matter mass is higher than the number ratio. This indicates that the reduction of PM number in the nucleation mode leads to a more noticeable reduction of total PM number than that of total PM mass.

Effects of Dilution Factor on the Catalytic VPR when sampling PM Emissions after a TWC. As explained in Section 2, the purpose of these tests is to see if the catalytic VPR could be used as an oxidation catalyst to reduce the particle number concentration. Only log-normal fitting data are used in the following analysis. The tests with nitrogen as a diluent (as opposed to air) enable the physical and chemical effects to be separated, and in order to separate out the dilution effect of the additional gas, a normalized specific PM emission has been

dx.doi.org/10.1021/es2008209 |Environ. Sci. Technol. XXXX, XXX, 000–000

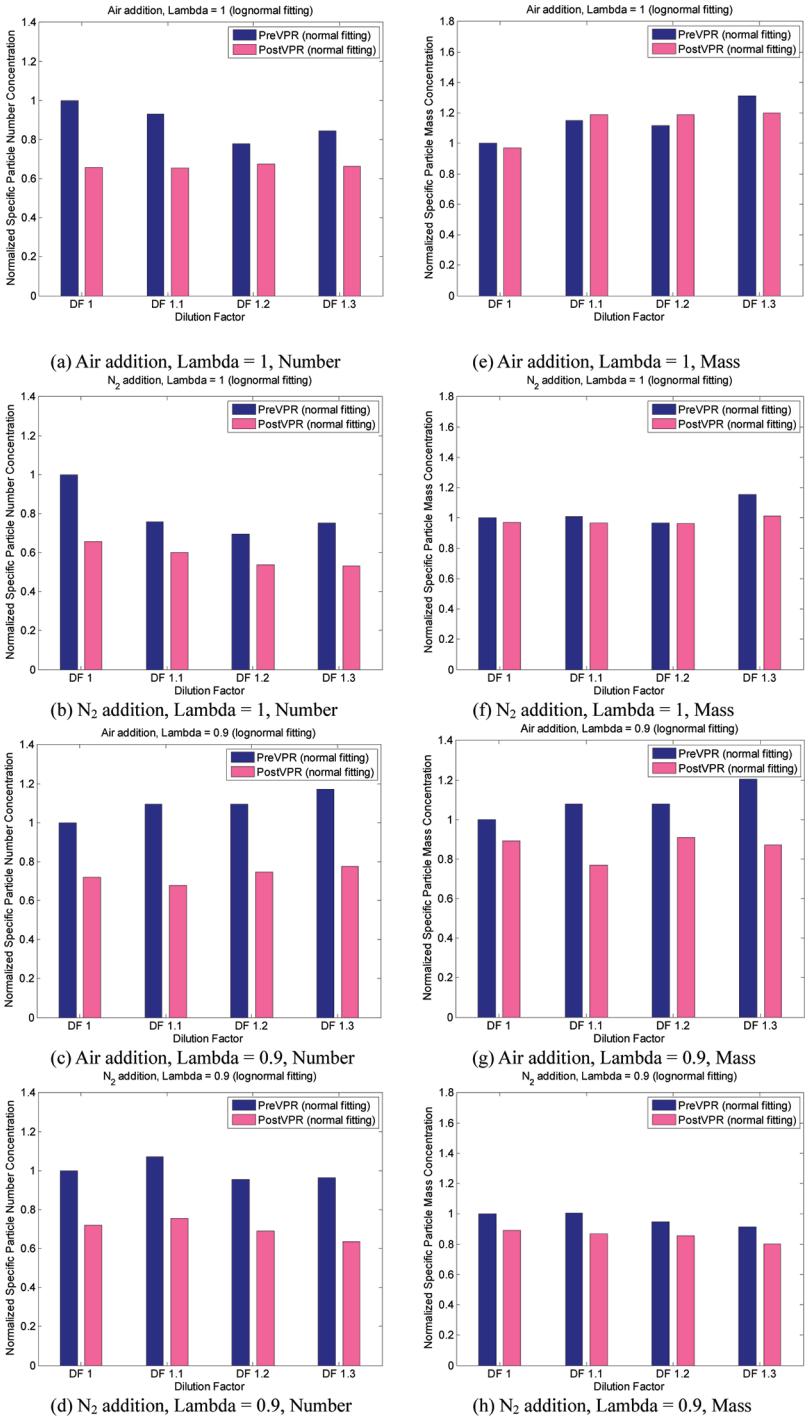

Figure 4. Normalized specific particle number and mass concentrations with either air or nitrogen addition and Lambdas of 1.0 and 0.9 (refer to Table 1 for the dilution factors) using eqs 8 and 9.

calculated. The normalized specific PM emission is defined as the post-VPR PM concentration times the corresponding VPR dilution factor (VPR-DF) then divided by the pre-VPR PM concentration derived from the log-normal fitting data when no dilution gas is added:

$$P_{\mathrm{n,\,norm}} = P_{\mathrm{n}} \times \text{VPR-DF}/P_{\mathrm{n,\,VPR\text{-}DF=1}} \quad (8)$$

$$P_{\mathrm{m,\,norm}} = P_{\mathrm{m}} \times \text{VPR-DF}/P_{\mathrm{m,\,VPR\text{-}DF=1}} \quad (9)$$

where $P_{\mathrm{n,norm}}$ represents normalized specific particle number emission, $P_{\mathrm{m,norm}}$ represents normalized specific particle mass emission, P_{n} represents particle number emission (no./cm^3), P_{m} represents particle mass emission (kg/cm^3), $P_{\mathrm{n,VPR\text{-}DF=1}}$ represents the particle number emission without dilution gas (no./cm^3), and $P_{\mathrm{m,VPR\text{-}DF=1}}$ represents the particle mass emission without dilution gas (kg/cm^3).

Figure S5 shows how increasing the dilution factor reduces the HC concentration by dilution, and it is for this reason that the PM emissions have been normalized by multiplying with the

dx.doi.org/10.1021/es2008209 |Environ. Sci. Technol. XXXX, XXX, 000–000

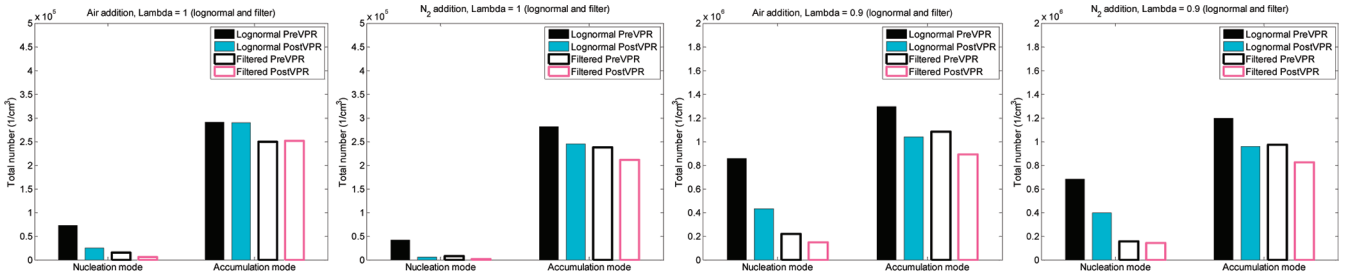

(a) Air addition, Lambda = 1 (b) N_2 addition, Lambda = 1 (c) Air addition, Lambda = 0.9 (d) N_2 addition, Lambda = 0.9

Figure 5. Particle numbers in different modes with a VPR dilution factor of 1.2 (refer to Table 1) obtained using log-normal fits to the pre- and post-VPR data and showing the effect of the PMP compliant digital filter.

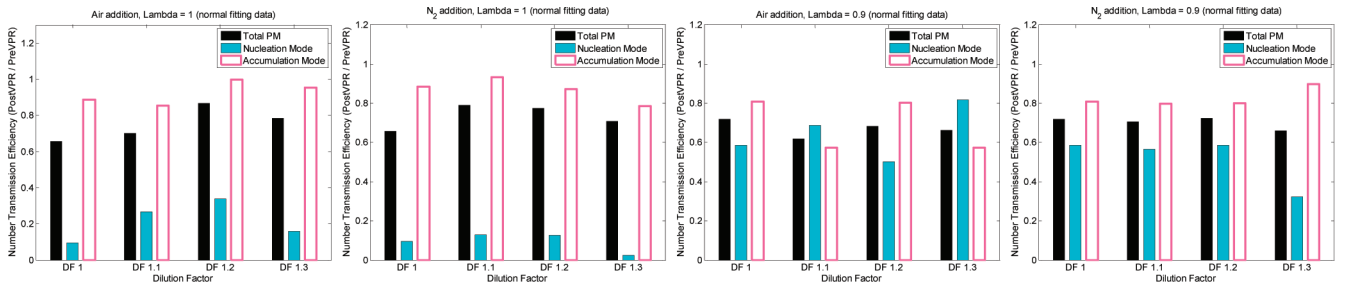

(a) Air addition, Lambda = 1 (b) N_2 addition, Lambda = 1 (c) Air addition, Lambda = 0.9 (d) N_2 addition, Lambda = 0.9

Figure 6. Number transmission efficiencies for different modes (total, nucleation, and accumulation) with either air or nitrogen addition and Lambdas of 1.0 and 0.9 (refer to Table 1 for the dilution factors).

dilution factor. However, when excess air is added it can be seen that hydrocarbon oxidation is very effective, so that any hydrocarbons desorbed from the PM will be oxidized.

Using eqs 8 and 9, Figure 4 shows the normalized specific total particle number and mass concentrations calculated from log-normal fitting to the data under various test conditions. Comparing the post-VPR with the pre-VPR particle emissions, there is a consistent reduction in the total number which is independent of the dilution factor, and this is more clearly seen with the rich mixture (Lambda = 0.9). The rich mixture gives a pre-VPR number concentration of typically 2.4×10^6 no./cm^3, and this is about 4 times the concentration at stoichiometric. The trend in the variation of the total mass pre- and post-VPR is less clear. For stoichiometric mixtures there is no change in mass, while for the rich mixture there is a reduction in mass. Since the reduction in mass occurs with dilution by either air or nitrogen, then this is a physical effect, not a chemical effect. This is further analyzed in Figure 5.

Data after normal fitting are used in Figure 5, where the data from Lambda = 0.9 with a dilution factor of 1.2 has been selected as a representative data set. The fitted log-normal data have been used, since this eliminates the effects of noise in the measurements. Because the European legislation prescribes the use of a VPR, this has been achieved numerically by using eq 5. Digitally processed measurements from the DMS500 have been compared with measurements made in conformance with the European Method for a range of different engine types (including spray guided gasoline), Braisher et al.,[6] and very good agreement was found. The nucleation mode particle number concentration is lower than the accumulation mode particle number concentration because the exhaust sample is after the TWC. As expected from eq 5, the reduction in the nucleation mode particle number concentration is greater than for the accumulation mode particles. Also, as would be expected from Figure 4 there is no difference between air and nitrogen as diluents. The effect of the numerical VPR (eq 5) is of course greatest for the nucleation mode particles and the difference between pre- and post-catalytic VPR is small after applying the numerical VPR. Further analyzing the total number ratio (post-VPR/pre-VPR) for the total PM, nucleation mode, and accumulation mode (Figure 6), it can be seen that at each measurement point for stoichiometric engine operation, the number ratios are in the following order: nucleation mode < total PM < accumulation mode; this is not always seen for the rich operation cases. Although the oxidation effect of the catalytic VPR has been verified by the HC results (Figure S5), it seems that when the engine was running rich of stoichiometric, the oxidation effects did not play much role in reducing the particle emissions. Apart from chemical reactions, some physical processes were taking place in the catalytic VPR as well.

The number transmission efficiencies are shown in the SI (Figure S6). It can be seen that the transmission efficiencies increase as the particle size increases, and the curves for the different engine Lambdas and additional gases are very similar above 10 nm. The engine IMEP was well controlled and this is shown in the Supporting Information (Figure S7).

4. DISCUSSION

The role of a catalytic VPR on engine particle emissions has been tested under different operating regimes with a DISI engine. The results can be summarized as follows.

(1) With the pre-TWC engine exhaust, nucleation mode particles constitute a large portion of the total particle number but only constitute a small portion of the total

dx.doi.org/10.1021/es2008209 |Environ. Sci. Technol. XXXX, XXX, 000–000

particle mass. The catalytic VPR led to a significant reduction in the particle number, especially the smaller size (nucleation mode) particles.

(2) The VPR temperature and exhaust residence time ($MFM_{exhaust}$) did not show much effect on the catalytic VPR performance once the $MFM_{exhaust}$ was above 0.09 g/s. The catalytic VPR transmission efficiencies for different size particles showed similar trends for the various VPR temperatures and $MFM_{exhaust}$ tested. Generally, the transmission efficiencies of the VPR follow the trends of the scaled PMP counting efficiency.

(3) When post-TWC exhaust was introduced to the catalytic VPR, it showed a moderate reduction effect on the number of particles. With a stoichiometric air−fuel ratio, the performance of the catalytic VPR was not affected by the use of additional air. Even with rich mixture combustion, there was still not a noticeable effect with increasing additional air on the catalytic VPR performance.

(4) For each air−fuel ratio, the transmission efficiency of the catalytic VPR did not change much with different types and varying amounts of additional gas. A comparison between adding air or nitrogen as a diluent showed that the reduction in particle number through the catalytic VPR is more likely to be due to physical than chemical processes.

■ ASSOCIATED CONTENT

Supporting Information. Table S1, Characteristics of the Test Engine; Figure S1, data filter (Wiebe function) described by eq 5; Figure S2, pre- and post-VPR temperatures with different mass flow rate of exhaust ($MFM_{exhaust}$) and different VPR temperatures; Figure S3, representative size distribution of raw data and its log-normal fitting; Figure S4, mass ratio (post-VPR/pre-VPR) for different modes (total, nucleation, and accumulation) for different sample flow rates ($MFM_{exhaust}$) and different VPR temperatures; Figure S5, HC emissions with either air or nitrogen addition under rich operation; Figure S6, number transmission efficiencies versus d_p with various gas additions and relative air−fuel ratios; Figure S7, pre- and post-VPR temperatures and the IMEP with air or nitrogen addition and relative air−fuel ratios of 1.0 and 0.9. This material is available free of charge via the Internet at http://pubs.acs.org.

■ AUTHOR INFORMATION

Corresponding Author

*Phone: +44 1865 283467; e-mail: fan.xu@eng.ox.ac.uk.

■ ACKNOWLEDGMENT

Jaguar Cars are thanked for the provision of the V8 engine and technical support.

■ REFERENCES

(1) Kittelson, D. B. Engines and Nanoparticles: A Review. *J. Aerosol Sci.* **1998**, *29* (5/6), 575–588.

(2) Maricq, M. M.; Posdiadlik, D. H.; Chase, R. E. Gasoline Vehicle Particle Size Distribution: Comparison of Steady State, FTP and US06 Measurements. *Environ. Sci. Technol.* **1999**, *33*, 2007–2015.

(3) Kasper, A.; Burtscher, H.; Johnson, J. P.; Kittelson, D. B.; Watts, W. F.; Baltensperger, U.; Weingartner, E. *Particle Emissions from SI-Engines During Steady State and Transient Operation Conditions*; SAE paper 2005-01-3136.

(4) Kittelson, D. B.; Watts, W. F.; Johnson, J. P.; Schauer, J. J.; Lawson, D. R. On-road and laboratory evaluation of combustion aerosols. Part 2: Summary of spark ignition engine results. *Aerosol Sci.* **2006**, *37*, 931–949.

(5) Ericsson, P.; Holmström, M.; Amberntsson-Carlsson, A.; Ohlson, C.; Skoglundh, M.; Andersson, B.; Carlsson, P. A. *Characterization of Particulate Emissions and Methodology for Oxidation of Particulates from Non-Diesel Combustion Systems*; SAE paper 2008-01-1746.

(6) Braisher, M.; Stone, R.; Price, P. *Particle Number Emissions from a Range of European Vehicles*; SAE paper 2010-01-0786.

(7) Geller, M. D.; Ntziachristos, L.; Mamakos, A.; Samaras, Z.; Schmitz, D. A.; Froines, J. R.; Sioutas, C. Physicochemical and redox characteristics of particulate matter (PM) emitted from gasoline and diesel passenger cars. *Atmos. Environ.* **2006**, *40*, 6988–7004.

(8) Zervas, E.; Dorlhène, P.; Forti, L.; Perrin, C.; Mornique, J. C.; Monier, R.; Ing, H.; Lopez., B. Interlaboratory Study of the Exhaust Gas Particle Number Measurement Using the Condensation Particle Counter (CPC). *Energy Fuels* **2006**, *20*, 2426–2431.

(9) Lee, H.; Kim, J.; Myung, C. L.; Park, S. Experimental investigation of nanoparticle formation characteristics from advanced gasoline and diesel fueled light duty vehicles under different certification driving modes. *J. Mech. Sci. Technol* **2009**, *23*, 1591–1601.

(10) Andersson, J.; Giechaskiel, B.; Muñoz-Bueno, R.; Sandbach, E.; Dilara, P. Particle Measurement Programme (PMP) Light-duty Inter-laboratory Correlation Exercise (ILCE_LD) Final Report; 54th GRPE, 4−8 June 2007, agenda item 3. GRPE-54-08-Rev.1.

(11) Giechaskiel, B.; Dilara, P.; Sandbach, E.; Andersson, J. Particle measurement programme (PMP) light-duty inter-laboratory exercise: Comparison of different particle number measurement systems. *Meas. Sci. Technol.* **2008**, *19*, 095401.

(12) Mathis, U.; Mohr, M.; Forss, A. M. Comprehensive particle characterization of modern gasoline and diesel passenger cars at low ambient temperatures. *Atmos. Environ.* **2005**, *39*, 107–117.

(13) Ristimäki, J.; Keskinen, J.; Virtanen, A.; Maricq, M.; Aakko, P. Cold Temperature PM Emissions Measurement: Method Evaluation and Application to Light Duty Vehicles. *Environ. Sci. Technol.* **2005**, *39*, 9424–9430.

(14) Ntziachristos, L.; Mamakos, A.; Samaras, Z.; Mathis, U.; Mohr, M.; Thompson, N.; Stradling, R.; Forti, L.; Serves, C. *Overview of the European "Particulates" Project on the Characterization of Exhaust Particulate Emissions From Road Vehicles: Results for Light-Duty Vehicles*; SAE paper 2004-01-1985.

(15) Graskow, B. R.; Kittelson, D. B.; Ahmadi, M. R.; , Morris, J. E. *Exhaust Particulate Emissions from a Direct Injection Spark Ignition Engine*; SAE paper 1999-01-1145.

(16) CONCAWE. *Comparison of Particle Emissions from Advanced Vehicles Using DG TREN and PMP Measurement Protocols*; Report 2/09; Brussels, 2009.

(17) Drake, M. C.; Fansler, T. D.; Solomon, A. S.; Szekely, G. A., Jr. *Piston Fuel Films as a Source of Smoke and Hydrocarbon Emissions from a Wall-Controlled Spark-Ignited Direct-Injection Engine*; SAE paper 2003-01-0547.

(18) Stojkovic, B. D.; Fansler, T. D.; Drake, M. C.; Sick, V. High-speed imaging of OH* and soot temperature and concentration in a stratified-charge direct-injection gasoline engine. *Proc. Combust. Inst.* **2005**, *30*, 2657–2665.

(19) Drake, M. C.; Haworth, D. C. Advanced gasoline engine development using optical diagnostics and numerical modeling. *Proc. Combust. Inst.* **2007**, *31*, 99–124.

(20) Schwarz, Ch.; Schünemann, E.; Durst, B.; Fischer, J.; Witt, A. *Potential of the Spray-Guided BMW DI Combustion System*; SAE paper 2006-01-1265.

(21) Abdul-Khalek, I. S.; Kittelson. D. B. *Real Time Measurement of Volatile and Solid Exhaust Particles Using a Catalytic Stripper*; SAE paper 950236.

(22) Kittelson, D. B.; Watts, W. F.; Savstrom, J. C.; Johnson, J. P. Influence of a catalytic stripper on the response of real time aerosol instruments to diesel exhaust aerosol. *J. Aerosol Sci.* **2005**, *36*, 1089–1107.

(23) ECE/TRANS/WP.29/GRPE/2008/page 62 Appendix 5. Particle Number Emissions Measurement Equipment.

(24) Khalek, I. *Sampling System for Solid and Volatile Exhaust Particle Size, Number, and Mass Emissions*; SAE paper 2007-01-0307.

(25) Khalek, I.; Bougher, T. *Development of a Solid Exhaust Particle Number Measurement System Using a Catalytic Stripper Technology*; SAE paper 2011-01-0635.

(26) Khalek, I.; Bougher, T.; Jetter, J. *Particle Emissions from a 2009 Gasoline Direct Injection Engine Using Different Commercially Available Fuels*; SAE paper 2010-01-2117.

(27) Sandford, M.; Page, G.; Crawford, P. *The All New AJV8*; SAE paper 2009-01-1060.

(28) Reavell, K.; Hands, T.; Collings, N. *A Fast Response Particulate Spectrometer for Combustion Aerosols*; SAE paper 2002-01-2714.

(29) Symonds, J.; Reavell, K.; Olfert, J.; Campbell, B.; Swift, S. Diesel soot mass calculation in real-time with a differential mobility spectrometer. *Aerosol Sci.* **2007**, *38*, 52–68.

(30) Symonds, J.; Price, P.; Williams, P.; Stone, R. Density of particles emitted from a gasoline direct injection engine. 12th ETH-Conference on Combustion Generated Nanoparticles, June 2008.